MEZCLA INDUCIDA POR GRAVEDAD EN UNA GEOMETRÍA CONFINADA

BUOYANCY DRIVEN MIXING IN CONFINED GEOMETRIES

T. Séon, Y. Tanino, J. Znaien, F. Moisy, JP Hulin, D. Salin.

Universidad Pierre et Marie Curie-Paris 6, Universidad Paris-Sur, CNRS, Laboratorio FAST, Bât. 502, Campus Universitario, Orsay F-91405, France
jean-pierre.hulin@u-psud.fr

Recibido: 20/12/2012; aceptado: 12/03/2013

Estudiamos la mezcla espontánea de dos fluidos con una diferencia de densidad caracterizada por el número de Atwood *At* y que ocupa inicialmente (en una configuración gravitacionalmente inestable) medio tubo inclinado en un ángulo θ respecto de la vertical. Para θ bajos y At altos, se observa un flujo turbulento que induce una mezcla eficiente a través de la sección del tubo; para θ altos y *At* bajos, el flujo es laminar y estratificado presentando tres capas de diferentes densidades o, inclusive una contracorriente viscosa de los fluidos. Para valores intermedios, se observan flujos intermitentes con secuencias de flujos laminares acelerando durante una fracción del tiempo creciente con θ. La estructura local del flujo y de la distribución de concentración han sido estudiados con PIV y LIF. En los regímenes de inercia, la velocidad de flujo se determina por el salto de concentración sobre el frente de desplazamiento. En el régimen turbulento, la velocidad varía linealmente en el diámetro del tubo, con un máximo de transferencia de cantidad de movimiento en el eje. Para θ crecientes y *At* decrecientes, el gradiente de concentración en el eje del tubo aumenta y aparecen canales de soluciones concentradas de cada fluido.

Palabras clave: turbulencia, mezcla, estratificación, intermitencia.

We study the spontaneous mixing of two fluids with a density difference characterized by the Atwood number *At*, and occupying initially (in a gravitationally unstable configuration) half of the length of a tube at an angle θ from vertical. At low θ and high *At* values, one observes a turbulent flow inducing an efficient mixing across the tube section; at high θs and low *At*'s, a stratified laminar flow with three layers of different densities appears or, even, a fully separated viscous counter flow. At intermediate values, intermittent flows are observed with sequences of accelerating laminar flows during a fraction of the time increasing with θ. The local structures of the flow and of the concentration distribution have been studied by PIV and LIF techniques. In the inertial regimes, the flow velocity is determined by the concentration contrast at the front. In the turbulent regime, the velocity varies linearly on the tube diameter with a maximum of momentum transfer at the axis. Increasing θ and decreasing *At* increases the concentration gradient at the tube axis and channels of concentrated solutions of each fluid appear.

Keywords: turbulence, mixing, stratification, intermittency.

I. INTRODUCTION

The coexistence of currents of fluids of different densities is very common in nature (oceanic flows, flows of particle or pollutant laden flows into a river or into the sea) as well as in the industry (chemical, petroleum or fire propagation). A particularly important case for practical applications is that of confined flows, for instance inside a channel: a key issue is whether the different fluids get mixed and to which extent. For instance, the completion of an oil well involves the separate injection of miscible fluids (cement slurry, drilling mud, washer fluids...) in the well: one wishes then to avoid mixing so that they retain their required properties. Related problems are gravity currents[1,2] (although the effect of confinement is generally weaker), lock exchange flows[3] and the Boycott effect.

In this paper, we study the spontaneous interpenetration and mixing of two fluids of different densities inside a long cylindrical tube: we discuss first global scale measurements of the front velocity and its dependence on the experimental parameters. Then, the local structure of the velocity and relative concentration fields is studied by LIF and PIV techniques.

II. EXPERIMENTAL PROCEDURE AND QUALITATIVE OBSERVATIONS

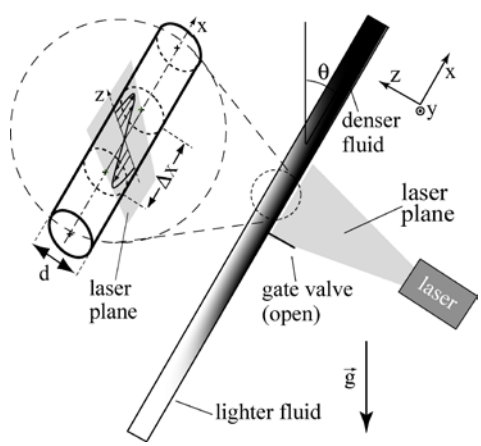

Figure 1 Experimental setup using a long, 20mm ID tube.

The experiments are performed inside a 4 m long perspex transparent tube of 20 mm inside diameter which can tilted all the way between vertical and

horizontal. Initially, each half of the tube length is filled by one of two miscible solutions with the denser one (water + salt) in the upper half and the lighter one (water with a light absorbing (or fluorescent) dye or fluorescent particles in the lower half. In some experiments, an equal amount of glycerol is added to the two fluids for varying the viscosity($10^{-3} < \mu < 4\ 10^{-3}$ Pa.s). A gate valve separates the two fluids and is opened at the initial time: flow is symmetrical with respect to the valve with fronts of light and heavy fluid respectively rising and descending at the same velocity.

The tube is illuminated by a fluorescent laser sheet located in a vertical diametral plane (Fig.1). The local relative mass concentration C of the two pure fluids in the mixture is determined from the fluorescence light intensity (LIF technique), using reference measurements with the tube filled by each of the pure fluids[6]. The velocity field is measured by the PIV technique[5].

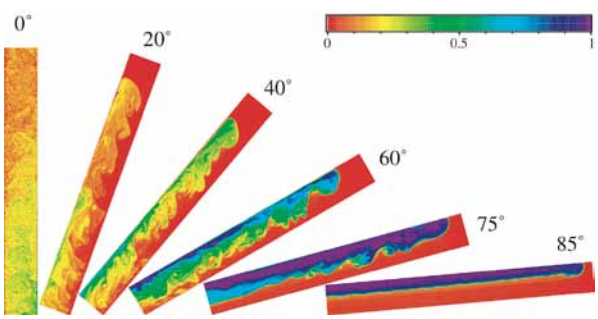

Figure 2. LIF maps of the relative concentration distribution in the vertical diametral plane of the tube at different tilt angles for At = 4 x 10^{-3} and a same viscosity $\mu = 10^{-3}$ Pa.s. Only a part of the tube length is shown: the field of view is 20 x300 mm. Red corresponds to the pure denser solution (C = 0) and purple to the lighter one (C = 1).

Typical relative concentration distributions determined by the LIF technique[6] in the vertical diametral plane of the tube are displayed in figure 2 for different tilt angles θ and a same density contrast between the two fluids characterized by an Atwood number value $At = (\rho_2 - \rho_1)/(\rho_2 + \rho_1) \cong \Delta\rho/2\rho = 4\ x\ 10^{-3}$ ($\Delta\rho$ is the density difference and ρ the average velocity). The interpenetration of the two fluids is due to the axial component of gravity: it creates a counter flow which may induce a Kelvin-Helmholtz instability mixing the two fluids across the section. The component $g \sin\theta$ of gravity transverse to the flow tends instead, except for $\theta = 0°$, to keep the two fluids separated with the lighter fluid in the upper part of the section. The competition between these two effects determines the flow pattern actually observed. For $\theta = 0°$, the variation of concentration at the front is continuous, the concentration distribution across the section is constant on the average and the flow is continuously turbulent. For $\theta = 20°$, a transverse concentration gradient is clearly visible, and a sharp concentration variation occurs at the front even though the flow remains turbulent. For $\theta = 60°$, some pure light fluid reaches the front and, for $\theta = 75°$, mixing occurs only in the center part of the section. Near horizontal ($\theta = 85°$), flow is laminar and no mixing occurs[7]. The reduced mixing at higher angles θ reflects the increasing influence of the transverse gravity.

III. FRONT VELOCITY VARIATIONS

Figure 3 displays the variation of the velocity V_f of the front of light fluid as a function of the tilt angle θ for the same Atwood number At = 4 x 10^{-3} as in Figure 2 (V_f is determined from the velocity of the boundary of the invaded zone in sequences of images like those of Fig. 2). At first, the front velocity increases with θ (regime 1)[4] while turbulence becomes visually weaker but remains continuous. Then, turbulence becomes intermittent while the increase of V_f levels off (regime 2). V_f becomes then constant with θ at a value V_{fmax}: in this regime 3, some mixing takes place right behind the front and the flow becomes then laminar. We shall not discuss here the final regime 4 in which V_f decreases with θ and which has been shown to be fully governed by the viscous forces.

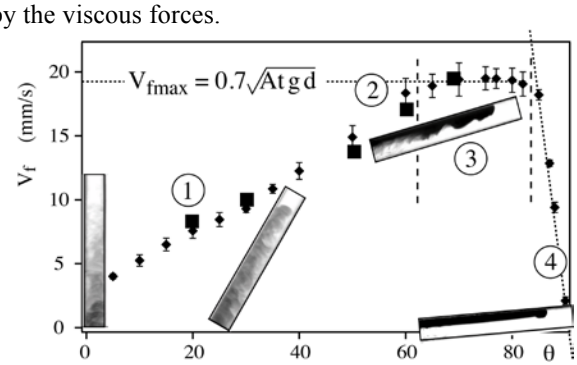

Figure 3. (♦) Variation of the front velocity V_f as a function of the tilt angle for the same experimental parameters as in Fig.2. (■) Front velocity estimated from equation (2).

Important additional information is obtained by studying the dependence of V_f on the viscosity μ (equal for the two fluids) and on the value of At. In regime 3, V_f is nearly independent of the viscosity and increases as $At^{1/2}$: moreover, one has :

$$V_f \simeq V_{f\max} = 0.7\sqrt{Atgd} = 0.7\sqrt{\Delta\rho/(2\rho gd)}\ .(1)$$

This latter expression and the lack of dependence on the viscosity μ suggest that V_f is determined by the balance between a buoyancy term $\Delta\rho\ g\ d$ and an inertial one ρV_f^2. Aside from the factor 0.7, this expression is the same as for other phenomena involving a similar balance like the velocity of gravity waves at the interface between thin layers of fluids of different densities or that of Taylor bubbles rising in large tubes.

In regime 1, V_f varies slowly with At and curiously increases with the viscosity μ: this latter feature is likely due to the reduced turbulence intensity (and mixing efficiency) as the viscosity increases (and, therefore, the Reynolds number decreases). This suggests to estimate V_f in this regime by replacing equation 1 by:

$$V_f \simeq 0.7\sqrt{\delta\rho/(2\rho gd)} = V_{f\max}\sqrt{\delta\rho/\Delta\rho} = V_{f\max}\sqrt{C_f}\ .(2)$$

in which C_f is the relative concentration at the rising front on the side of the light fluid ($C = 0$ on the other side so that the relative density contrast $\delta\rho/\Delta\rho$ is equal to C_f. In order to check this hypothesis, we plotted in figure 3 (■) symbols) the theoretical estimations of V_f

from equation (2) using the values of C_f at the front provided by the LIF maps of figure 2[6]. The very good agreement with the experimental values demonstrates that, in regimes (1)-(3), the velocity at the front is determined by the local concentration at the front which, itself, depends on the efficiency of turbulent mixing in the region between the fronts.

The type of flow regime observed does not depend only on the angle θ, but also on the density contrast: at higher *At* values, more energy is input into the turbulent mixing flow: the range of θ values over which the continuous turbulent regime is observed becomes broader and the maximum front velocity V_{fmax} is reached at higher angles from vertical. The physics of these phenomena is discussed in detail in other papers[5-9].

IV. LIF AND PIV MEASUREMENTS OF THE LOCAL VELOCITY AND CONCENTRATION

In order to understand the above results on the macroscopic front velocity, it is necessary to know better the properties of the flow at the local scale which is achieved by means of LIF and PIV measurements[5,6,8].

Laminar regime

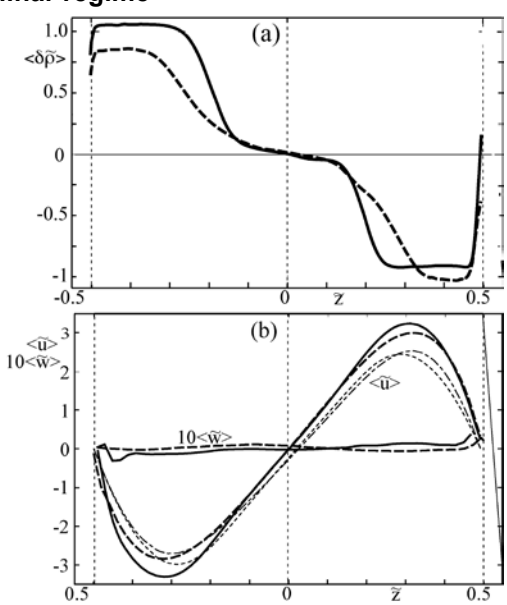

Figure 4 Transverse profiles of (a) the normalized local mean density contrast $\langle\delta\tilde{\rho}\rangle$ and (b) of the normalized mean longitudinal and transverse velocities $\langle\tilde{u}\rangle$ and $\langle\tilde{w}\rangle$ as a function of the transverse distance $\tilde{z}$ to the tube axis in the laminar flow regime for θ =45° (dashed lines) and θ = 60° (continuous lines) with At =10^{-3}. $\langle\tilde{w}\rangle$ is magnified vertically by a factor of 10. Thin dashed-dotted and dotted lines in (b): prediction of the mean velocity $\langle\tilde{u}\rangle$ from the density profiles.

Figure 4a displays the variation of the normalized local deviation of the density $\langle\delta\tilde{\rho}\rangle = 2(\langle\rho\rangle - \langle\rho\rangle_z)/\Delta\rho$ in which the average $\langle\rho\rangle_z$ is taken over the diameter. The measurement is taken far enough from the front (10 tube diameters and more) that the initial mixing behind the front has stopped. One observes (particularly clearly for θ =60°) a three steps variation of the concentration so that one has a layer of a mixture of the two fluids between two parallel layers of pure fluids. No velocity fluctuations are detectable and the transverse velocity $\langle\tilde{w}\rangle$ (normalized by the characteristic velocity $V_t = \sqrt{Atgd}$) is nearly zero. One has therefore a parallel viscous counter flow of the two fluids with a nearly linear variation of the longitudinal velocity *u* with the distance *z* in the center part. This flow profile is well predicted by numerical simulations (dotted and dashed dotted lines) assuming a parallel Stokes flow in the tube section. As the angle θ increases, the width of the mixed layer becomes narrower until it disappears and one has only a counter flow of the two pure solutions.

Continuous turbulent regime

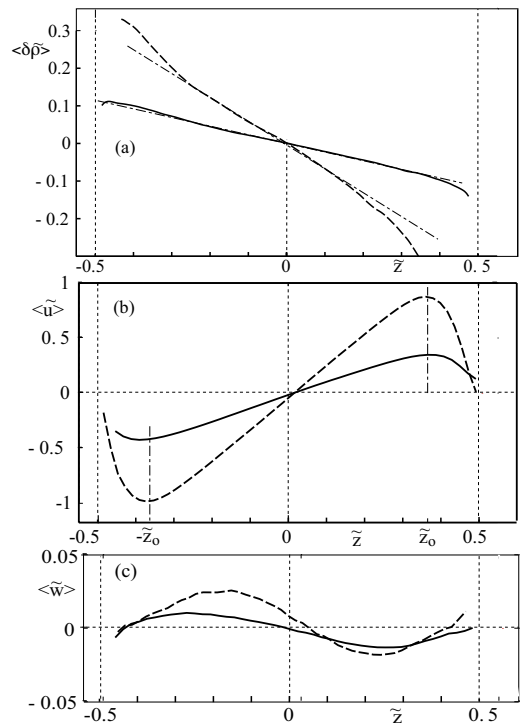

Figure 5. Transverse profiles of (a) the normalized local mean density contrast $\langle\delta\tilde{\rho}\rangle$ and of the mean longitudinal (b) and transverse (c) velocities $\langle\tilde{u}\rangle$ and $\langle\tilde{w}\rangle$ as a function of the transverse distance $\tilde{z}$ to the tube axis in the continuous turbulent flow regime for θ =15°and At = 10^{-2} (continuous lines) and θ = 60° and At = 4 x 10^{-3}(dashed lines). Thin dashed-dotted and dotted lines in (a) : slope at the origin.

In the continuous turbulent regime, the variation of $\langle\delta\tilde{\rho}\rangle$ with the transverse distance $\tilde{z}$ is linear with a very small gradient at high *At* and low θ values (figure 5a): in this case, the turbulent strength is highest and turbulent mixing is effective across the whole tube section (continuous line). At lower *At* and higher angles θ, the density varies linearly with $\tilde{z}$ only in the center part of the tube (dashed line in figure 5a); the density gradient increases near the walls, due to higher concentration channels visible in figure 2.

Like the front velocity V_f, the mean axial velocity $\langle\tilde{u}\rangle$ is lower for the most strongly turbulent flow, due to better mixing resulting in a lower concentration contrast at the front. The variation of $\langle\tilde{u}\rangle$ with the distance $\tilde{z}$ is remarkably linear in the center of the pipe over most of the diameter while, near the walls, the velocity gradient is large. The transverse component $\langle\tilde{w}\rangle$ is about 40 times lower than $\langle\tilde{u}\rangle$ but is not negligible (figure 5c): numerical simulations show that it corresponds to the

occurence of a secondary flow with 4 recirculation cells of alternate directions in the section of the tube[5,9].

Momentum transfer in this flow differs strongly from that in pressure driven turbulent flows in channels (figure 6). First, the turbulent Reynolds stress term is highest on the axis and becomes small in the vicinity of the maximum of the mean velocity ($\tilde{z} = \pm\tilde{z}_0$): actually, the flux of momentum generally takes place between the two parts of the tube where the fluid flows in opposite directions and not between the fluid and the walls like in pressure driven channel flows (there is only momentum flux towards the walls close to them, *i.e.* for $\tilde{z} > \tilde{z}_0$)[5].

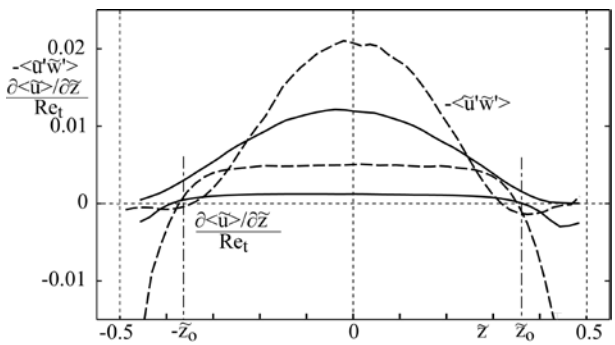

Figure 6: Turbulent (top curves) and viscous (bottom curves) in-plane normalized stress components for the same cases as in figure 5. Vertical dashed-dotted lines are the location of the extrema of the mean velocity.

The turbulent Reynolds stress term is significantly larger than the viscous one in the center part of the tube: the contrast between the two terms is however larger in the most turbulent case The viscous stress becomes dominant in the wall region for $\tilde{z} > \tilde{z}_0$ while the turbulent stress may change sign. Measurements of the transverse velocity fluctuation also display a similar maximum on the tube axis.

Intermittent turbulent regime

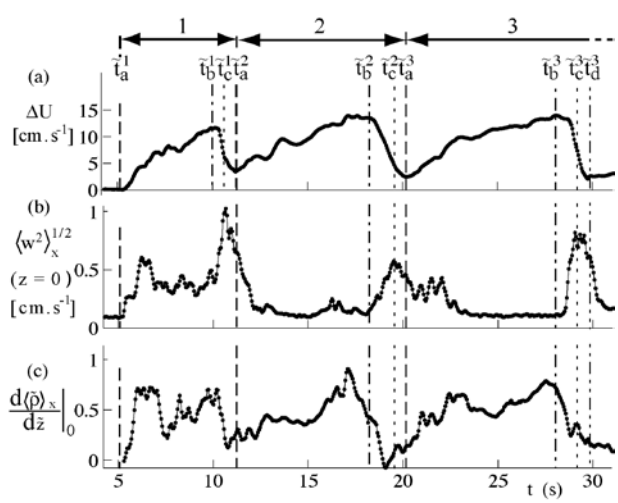

Figure 7: Time variation in the intermittent regime of : (a) the velocity difference ΔU_M = Umax - Umin; (b) the root mean square of the transverse velocity fluctuations w; (c) the normalized concentration gradient on the axis of the tube. Experimental parameters : At = 2.55 10^{-3}; θ = 45°.

At intermediate values of θ and *At,* the transition from the turbulent to the laminar regime takes place continuously through the appearance of phases of laminar flow of duration increasing with θ[10].

Three such sequences are shown in Figure 7. Starting at a time t_a at which the fluid is well mixed, the fluid accelerates (curve 1) until a turbulent burst appears between times t_b and t_c : then, the turbulent fluctuations increase (curve b) and the transverse density gradient (curve c) is smaller. The mean flow slows down and a new sequence may start again. Turbulent bursts occur when the local Reynolds number $Re = \Delta U_M d/\nu$ becomes of the order of 2300 ($\Delta U_M = U_{max}$ - U_{min} in the profile); this implies a strong influence of the viscous forces[10] so that classical stability criteria for stratified flows based on the value of the Richardson number are not valid.

V. CONCLUSION

These results demonstrate the very specific features and the diversity of these confined counter flows driven by the density difference between the two fluids.

These flows are characterized by a strong coupling between the shear flow in the mixing zone between the fronts and the velocity V_f of the latter. The mixing flow controls indeed the density variation at the front which, in turn, determines the velocity V_f. In order to insure mass conservation, the value of V_f limits in turn the maximum velocity reached in the mixing zone.

In the laminar case, for instance, the thickness of the mixed central layer adjusts itself so that the corresponding flow rate matches that in the region of the front. In the strongly turbulent case, the lower front velocity is paralleled by low values of both the maximum velocity and the transverse density gradient in the mixing zone. For more weakly turbulent flows, weaker mixing results in an increase of the mean velocities and concentration gradient and in the appearance of channels of concentrated solutions in the upper and lower parts of the flow section.

Acknowledgments

We thank M. Debacq, Y. Hallez, E.J. Hinch, J. Magnaudet and B. Perrin, for their collaboration and A. Aubertin, C. Borget and R. Pidoux.for their technical assistance. This work has been supported by the Agence Nationale pour la Recherche grant 07-BLAN-0181.

VI. REFERENCES

1 - T. B. Benjamin, J. Fluid Mech. 31, 209 (1968).
2 - P. Odier, J. Chen, M. K. Rivera, and R. E. Ecke, Phys. Rev. Lett. 102, 134504 (2009).
3 - J. O. Shin, S. B. Dalziel and P. F. Linden, J. Fluid Mech. 521, 1 (2004).
4 - T. Séon, D. Salin, J. P. Hulin, B. Perrin and E. J. Hinch, Phys. Fluids 17, 031702 (2005).
5 - J. Znaien, Y. Hallez, F. Moisy, J. Magnaudet, J. P. Hulin, D. Salin, and E. J. Hinch, Phys. Fluids 21, 115102 (2009).
6 - T. Séon, J. P. Hulin, D. Salin, B. Perrin and E. J. Hinch, Phys. Fluids 18, 041701 (2006).
7 - T. Séon, J. Znaien, D. Salin, J. P. Hulin, E. J. Hinch, and B. Perrin, Phys. Fluids 19, 123603 (2007).
8 - J. Znaien, F. Moisy and J. P. Hulin, Phys. Fluids 23, 035105 (2011).
9 - Y. Hallez and J. Magnaudet, Phys. Fluids 20, 053306 (2008).
10 - Y. Tanino, F. Moisy and J. P. Hulin, Phys. Rev. E 85, 066308 (2012).
11 - A. Defina, S. Lanzoni, and F. M. Susin, Phys. Fluids 11, 344 (1999).